

Induction of a biaxial nematic phase by means of an electric field

R. Stannarius¹, A. Eremin¹, M.-G. Tamba², G. Pelzl², W. Weissflog²,

¹ Otto-von-Guericke-University, Institute of Experimental Physics, Universitätsplatz 2, D-39106 Magdeburg, email: ralf.stannarius@physik.uni-magdeburg.de

² Martin-Luther-University Halle, Institute of Physical Chemistry, Mühlpforte 1, D-06108 Halle, email: weissflog@chemie.uni-halle.de

It is demonstrated in electro-optic experiments that a uniaxial nematic phase of a bent-core mesogen can be switched into an optically strongly biaxial state by means of an external electric field of the order of 10^5 V/m. The metastable biaxial state is identified by its optical and electric properties. After the field is switched off, uniaxial and biaxial domains can coexist for about one hour. During this time, the biaxial domains gradually shrink but they can be stabilized in moderate electric fields. The formation of inversion walls inside the biaxial domains in the planar ground state, as well as the occurrence of such domains in homeotropic cells evidence that the biaxiality is not imposed by the boundary conditions of the planar cell.

1 Introduction

Bent-shaped mesogens are known to exhibit numerous liquid crystalline mesophases, including many layered and columnar structures. For sterical reasons, they are less suited to form a nematic phase, the bent shape of the molecules favours layered or other positional packing. Nevertheless, several successful strategies to produce nematic phases of bent-core mesogens have been reported [1, 2, 3, 4, 5, 6, 7]. The tendency for molecular positional order is smaller for example when the bending angle of the 'banana-shaped' molecule is increased towards a stretched angle by lateral substituents at the central phenyl ring [2]. Nematic phases are also found in mixtures of calamitic and bent-core mesogens [5]. The material studied here is a twin mesogen with a bent-core subunit covalently bound to a rod-like part by a flexible spacer [7], its chemical structure is shown in Fig. 1.

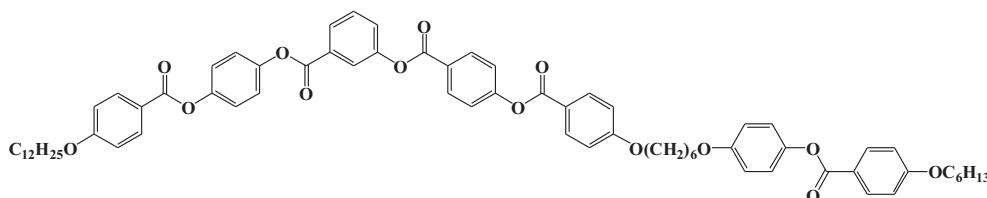


Figure 1: Chemical structure of the investigated mesogen. The phase sequence is Cr 160 (Col 149) N 167.5 I [7].

In smectic phases formed by bent core mesogens, electric fields can induce structural changes, for example the switching of the phase chirality. Domains of different chirality can

coexist, and switching processes may even compete in one sample, e.g. one preserving the chirality of the molecular arrangement, the second converting it [8], depending on temperature and frequency, but also on the applied field strength. Domains of opposite chirality may grow or shrink in dependence on the direction of the applied electric field, and even the phase transition from the isotropic phase into a mesophase with spontaneous polarization may be reversibly controlled by means of electric fields [9, 10]. Nematic phases, owing to the absence of long range positional order, are characterized by additional degrees of freedom of the director \hat{n} . Consequently one finds other prominent influences of the bent-core molecular geometry on physical properties, in both quantitative and qualitative aspects. An example is the discovery of a giant bend flexoelectric coefficient e_{33} in a bent-core nematic [11]. Novel types of electrically driven convection structures have been described [12]. The electro-optic behaviour of sandwich cells filled with bent-core nematics is substantially different from that of calamitic nematics [13].

Their sterical shapes qualify bent-core nematogens as potential candidates for biaxial order. Biaxial nematic phases have been long sought with little success in calamitic thermotropic materials. Since the discovery of biaxial lyotropic nematics [14], there have been numerous efforts to find biaxiality in thermotropic nematics, using a variety of experimental techniques. Finally, biaxial nematics of bent-core mesogens have been identified by NMR and X-ray methods [15, 16, 17].

The purpose of this report is to present convincing evidence from electro-optical experiments that in a sufficiently strong external electric field, one can transform the uniaxial phase of the mesogen in Fig. 1 into a metastable biaxial state, either in the complete cell or in domains coexisting with domains in the original uniaxial state. We provide arguments that the biaxial state is not imposed by boundary conditions of the cell but represents a thermodynamically metastable biaxial phase.

We use a commercial sandwich cell (E.H.C.) with a cell gap of $d = 25 \mu\text{m}$ and rubbed polyimide coating of the glass plates for planar surface alignment. The cell is observed in transmission with a high-resolution cooled CCD camera AxioCam HR mounted on an AxioImager polarizing microscope (Carl Zeiss GmbH). All experiments are performed in monochromatic light ($\lambda = 532 \text{ nm}$), between crossed polarizers (vertical and horizontal in the images). Temperature is controlled with a Linkam LTS 350 heating stage. If not otherwise indicated, data refer to a temperature 7.5 K below the clearing point T_{NI} . The ac voltages (1 kHz) are synthesized with a TGA 1241 (TTi) function generator connected to a broadband amplifier.

The available amount of material was too small to measure dielectric constants or refractive indices, but the splay Fréedericksz transition (FT) evidences that the dielectric anisotropy $\Delta\varepsilon = \varepsilon_{\parallel} - \varepsilon_{\perp}$ is positive [13]. The study of the splay FT in an electric field applied normal to the glass substrate [18] reveals the following unexpected effect: When the applied field strength is sufficiently large (a few hundred kV/m to 1 MV/m), a transition into a certain new state of order takes place, which after the removal of the field leads to an altered ground state. This state differs optically from the planar ground state of the original, uniaxial nematic phase (N_{u}). The so far unidentified new state is designated here as N_{b} , with the following fundamental properties: The direction of the largest refractive index of N_{b} in the cell plane is unchanged with respect to the optic axis of N_{u} . The effective birefringence in the off state is reduced by about 15%. With a compensator we measure a

drop of $\Delta n = n_e - n_o = 0.136$ in N_u to $\Delta n' = \Delta n - \delta n = n_1 - n_2 = 0.115$ in N_b . Here, n_e and n_o are extraordinary and ordinary refractive indices of N_u , while n_1, n_2 are the corresponding effective refractive indices in N_b , for normally incident light polarized \parallel and \perp to the alignment axis, resp.

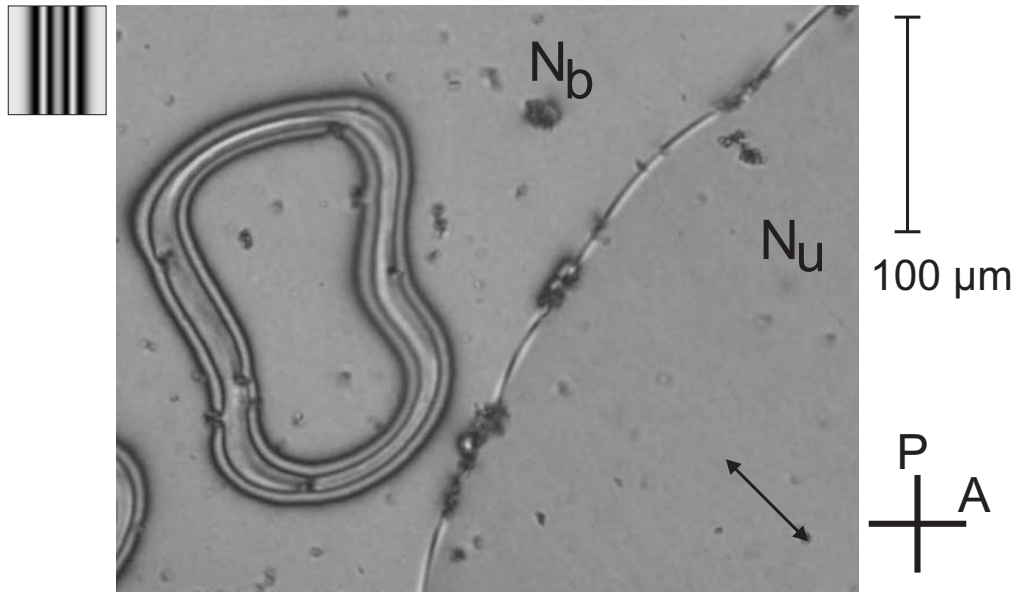


Figure 2: Two coexisting domains in the N_b (left) and N_u (right) planar ground states at zero field. The N_b domain contains a closed inversion wall loop. The director easy axis \hat{n} is in the direction of the arrow, the image in the top left corner is a texture simulation of a wall of the second director \hat{n}_2 (see text) in the N_b state.

It is possible to transform the complete region under the cell electrodes into the new state, but one can also obtain textures where N_u and N_b domains coexist, as shown in Figs. 2 and 3. These domains are separated by sharp borders which have not the appearance of walls but of either defect lines or phase boundaries. In such situations, the N_b domains shrink slowly when the electric field is off. After approximately one hour, the uniform N_u ground state is re-established in the whole cell. One can, however, reverse the regression of N_b domains by applying a sufficiently strong electric field. It is a mere coincidence that both states appear almost equally bright at 7.5 K below T_{NI} (Fig. 2), the order of interference being 6.4 and ≈ 5.4 , respectively. At other temperatures, the ratio of Δn to $\Delta n'$ remains approximately the same, so that at about 0.5 K below T_{NI} the N_u domains are near to a transmission maximum (half integer order $\Delta n d/\lambda$) while N_b domains are close to a minimum (integer $\Delta n' d/\lambda$).

N_b domains often contain walls in the off state (Fig. 2), in contrast to N_u domains which always relax to a uniform planar texture even if Brochard-Leger (BL) walls [19] had formed during the FT. The walls in the N_b ground state have width that are nearly independent of their orientations. This distinguishes them from the BL walls [13] in N_u . Moreover, they appear when the cell is switched off, irrespective of whether the tilted state above the FT was uniform or not (Fig. 3), and they disappear again above the Fréedericksz threshold. The walls often form closed loops that shrink on the time scale of minutes. Sometimes they are

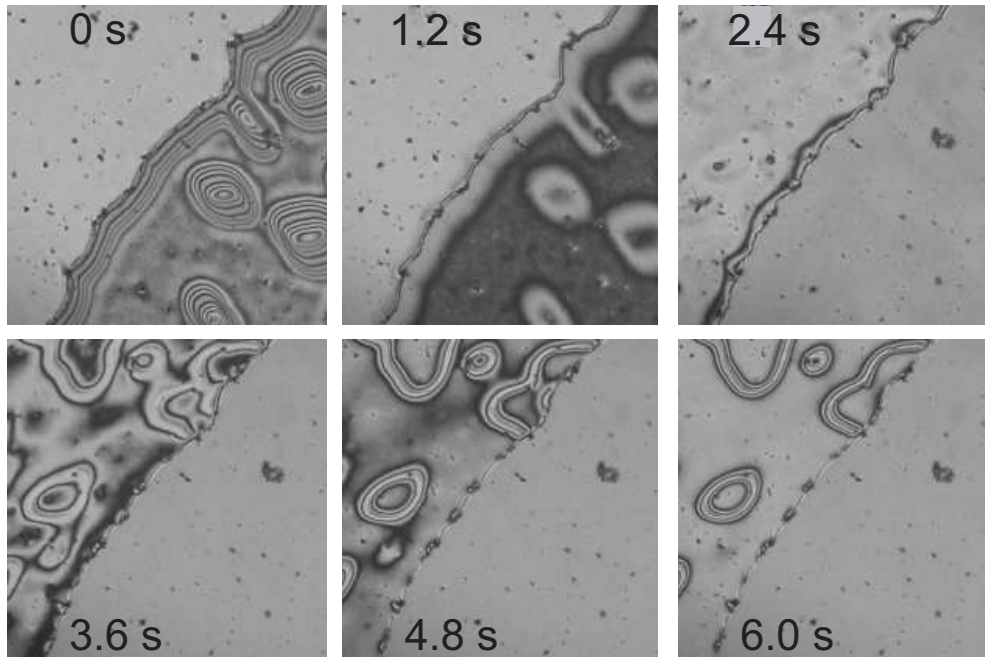


Figure 3: Same domains as in the previous figure after a voltage of 7.35 V has been switched off. The images are taken in 1.2 s intervals. In the N_u domain (bottom right), the BL walls disappear and the sample relaxes to the all-planar state while in the N_b domain (top left) a new type of walls appears in the off state. Image sizes $546 \times 546 \mu\text{m}^2$.

pinned with their ends at the borders of the N_b domain, then they may persist during the lifetime of the domain. Their optical profile at 7.5 K below T_{NI} consists of four dark zones, separating bright zones, the effective birefringence changes from $\Delta n - \delta n$ to $\Delta n + \delta n$ and back across the wall. Optical textures on both wall sides are indistinguishable.

Fig. 4 sketches schematically the state diagram of N_u in the $25 \mu\text{m}$ cell in the field strength - frequency parameter space. The FT has the lowest threshold, nearly frequency-independent. Above, there is the transition into a periodically distorted state (presumably electroconvection) and, after further instabilities, into a dynamic scattering (DS) regime. Details of the electro-optic characteristics of N_u are described in Ref. [13]. A similar behaviour is found in N_b domains, with different thresholds. If one chooses path (1), the transition $N_u \rightarrow N_b$ appears in the turbulent DS pattern and the transformation itself is difficult to identify. Varying the field along path (2), one can observe the nucleation of N_b domains, preferentially inside BL walls. Fringes in the optical profile of the original BL wall, Fig. 5a, evidence the continuous director rotation across the wall [19, 13] in N_u . The change in Fig. 5b reflects the transformation into an N_b domain, which later expands into adjacent N_u areas (Fig. 5c).

We interpret all experimental observations with the assumption that the electric field induces a transition into a biaxial nematic phase N_b that is metastable at zero field. N_b has refractive indices $n_1 \approx n_e$ (along the first director, \hat{n}_1), $n_2 = n_o + \delta n$, and $n_3 = n_o - \delta n$ (along the vertical axes \hat{n}_2, \hat{n}_3). If one assumes e.g. $n_o = 1.5$, the corresponding values are $n_1 = 1.636$, $n_2 = 1.521$, $n_3 = 1.479$. This yields an angle between the two optical axes of

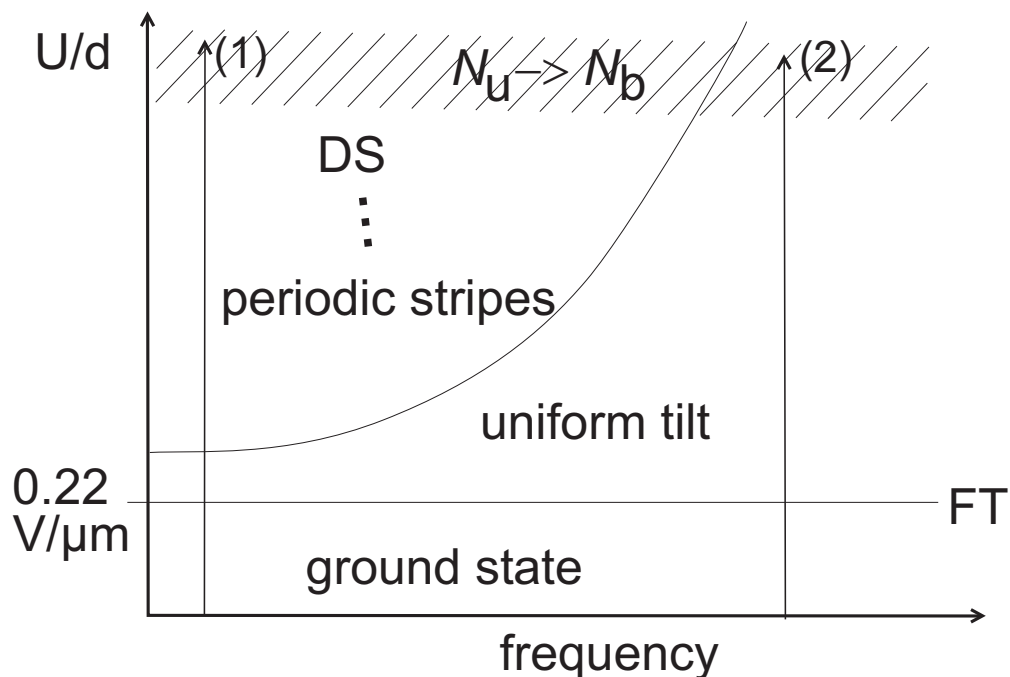


Figure 4: Schematical sketch of the N_u orientational states in a $25 \mu\text{m}$ cell in the voltage-frequency space. The transition to N_b is indicated. Arrows (1),(2) are explained in the text.

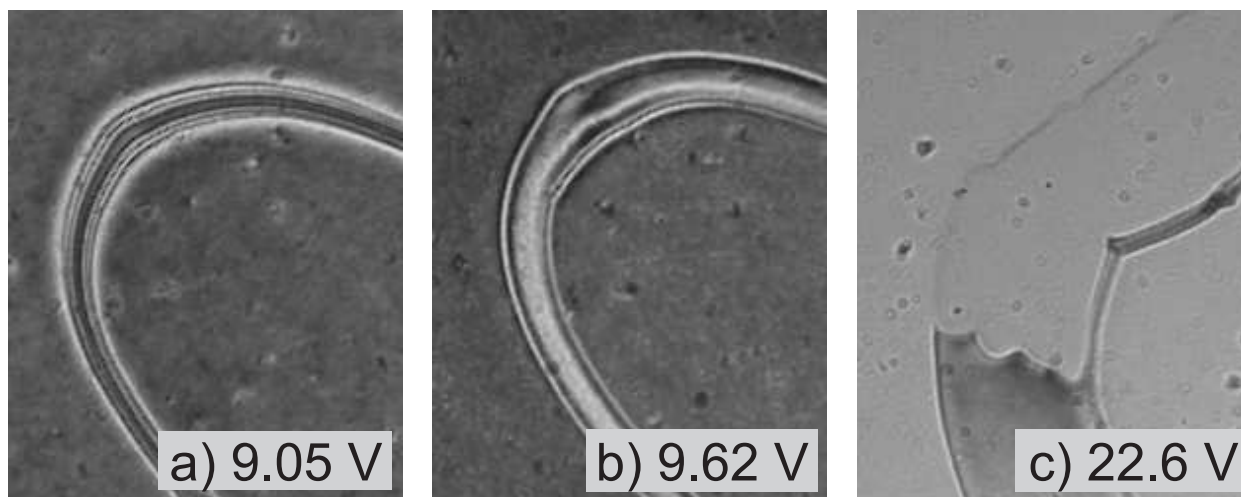


Figure 5: a) Texture of a BL wall in the N_u phase at 9.05 V. b) an N_b domain replaces the wall at a voltage of 9.62 V ($0.385 \text{ MV}/\text{m}$). c) 22.6 V, the same N_b domain expands into the surrounding N_u region. Image sizes $106 \mu\text{m} \times 132 \mu\text{m}$, $T = T_{\text{NI}} - 0.5 \text{ K}$.

66°. The comparably large optical biaxiality, $2\delta n = (n_2 - n_3) = 0.042$ evidences that the order parameter for the second director is fairly large.

In N_b the first director \hat{n}_1 is strongly anchored in rubbing direction, and the second director \hat{n}_2 is weakly anchored planarly, perpendicular to \hat{n}_1 . When the field is switched off, the first director relaxes to the all-planar undistorted state, while \hat{n}_2 is planar within domains that are separated by \hat{n}_2 inversion walls (Figs. 2,3). Their segments they can be classified into \hat{n}_2 splay-bend and \hat{n}_2 twist types (Fig. 6). For a calculation of the wall profiles, one-constant approximation that neglects the elastic anisotropy is a reasonable first estimate. It leads to the ansatz for the free energy per cell area $f = \frac{1}{2}Kd(d\varphi/dx)^2 - W \sin^2 \varphi$, with the coordinate x perpendicular to the wall, the tilt angle φ of \hat{n}_2 , the surface anchoring energy $\frac{1}{2}W \sin^2 \varphi(x)$ and an elastic constant K for \hat{n}_2 . We assume that there is no variation of \hat{n}_2 normal to the cell plane in the off state. One obtains the solution $\varphi = 2 \arctan(\exp(x/\xi))$ with $\xi = \sqrt{Kd/(2W)}$, and $n_{2,\text{eff}} = n_2 n_3 / \sqrt{n_3^2 \cos^2 \varphi + n_2 \sin^2 \varphi}$ replaces n_2 in the transmission characteristics. Across the wall, the interference order $\phi = (n_e - n_{2,\text{eff}})d/\lambda$ changes from approximately 5.4 (near the fifth maximum) through two minima and one maximum towards $\phi \approx 7.4$ (near the seventh maximum) in the center. A value of $\xi = 18 \mu\text{m}$ gives the optical image in the top left corner of Fig. 2, in satisfactory agreement in particular with the twist sections, top left and bottom right, of the experimental \hat{n}_2 inversion wall loops. This corresponds to a ratio $K/W \approx (25 \pm 5) \mu\text{m}$. If the anchoring of \hat{n}_2 were strong, one would find a pair of disclination lines at the glass substrates instead of the continuous wall.

When an electric field is applied, the second director aligns towards \vec{E} as shown in Fig. 6c, and the walls disappear. Two reorientation processes take place concurrently, the rotation of \hat{n}_2 into the normal direction and the FT of \hat{n}_1 .

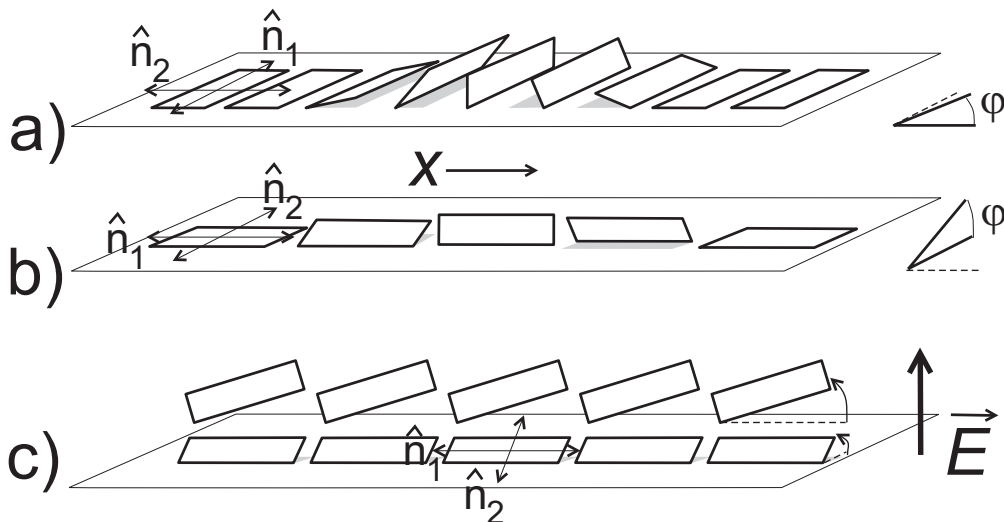


Figure 6: Sketch of the two types of inversion walls of the second director \hat{n}_2 in the biaxial phase in a cell with strong planar anchoring of \hat{n}_1 and weak anchoring for \hat{n}_2 . a) splay-bend wall, $\hat{n}_1 \perp x$, b) twist wall, $\hat{n}_1 \parallel x$. c) Alignment of \hat{n}_2 and FT of \hat{n}_1 in an electric field.

The FT threshold field in N_b is reduced by a factor of ≈ 2 respective to N_u . When we assume that the splay constant for the first director is unchanged, an effective dielectric

anisotropy $\varepsilon_{11} - \varepsilon_{33}$ increased by this factor respective to $\Delta\varepsilon$ can explain the threshold drop¹. Above the FT, the characteristics of N_b and N_u are comparable, when the voltage scale is scaled appropriately. Inversion walls of \hat{n}_2 disappear in the tilted director field, but they reappear at random positions when the field is off and \hat{n}_1 becomes planar again (Fig. 3).

The model also explains why the transition $N_u \rightarrow N_b$, path (2) in Fig. 4, occurs first in BL wall centers. There, \hat{n} remains planar, i.e. perpendicular to the field \vec{E} , even at high voltages [13] and consequently the electric forces acting towards an induction of order of the second axis are most effective. After its nucleation, the N_b domain is surrounded by a sharp border where lateral elastic torque is interrupted (Figs. 5b,c). The fringes that evidence a continuous deformation of the \hat{n} director across the BL wall [19, 13] disappear. The N_b domain switches into a highly tilted state, where the first director \hat{n}_1 reorients towards \vec{E} so that \hat{n}_2, \hat{n}_3 tilt away from \vec{E} . The ordering influence on \hat{n}_2 thus decreases, but the N_b domain, once nucleated, grows on the expense of the adjacent uniform N_u region. When the transformation occurs in the turbulent DS state (path (1) in Fig. 4), the director is randomly oriented and the electric field induces the N_b state in random domains that grow by coalescence. The threshold for the initiation of the N_b state is difficult to detect there but is apparently higher than along path (2).

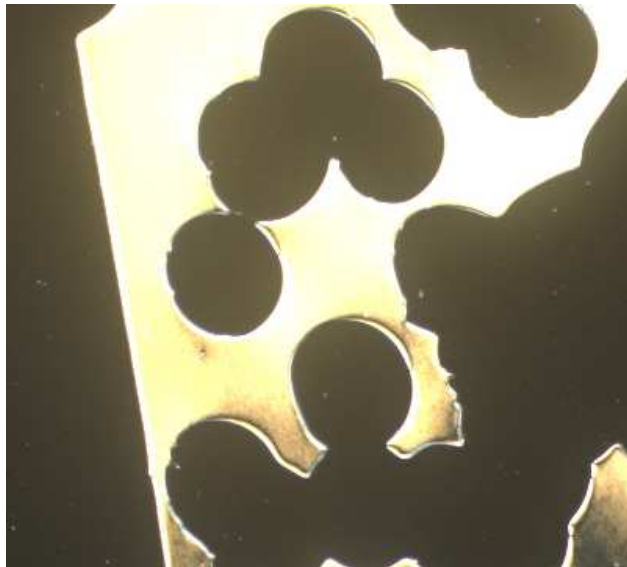


Figure 7: Biaxial nematic phase N_b in a $5 \mu\text{m}$ homeotropic cell, with enclosed circular domains of the uniaxial N_u phase, image size $424 \mu\text{m} \times 382 \mu\text{m}$. The temperature is somewhere between T_{NI} and $T_{\text{NI}} - 7.5 \text{ K}$. The sample has been exposed to an electric field above 10 MV/m at $T_{\text{NI}} - 7.5 \text{ K}$ for a few seconds. It undergoes a transition $N_u \rightarrow N_b$ and heats up uncontrolled due to dissipation. After the field is switched off, the area under the electrodes is in the N_b state and exhibits a Schlieren texture under crossed polarizers. The interference order $(n_2 - n_3)d/\lambda$ is near the first maximum. Outside the electrode area (left in the image), the sample is still N_u . Within the N_b region, N_u domains start to grow quickly from random locations.

Strictly, the experiment has not proven that the biaxial state N_b is a thermodynamic phase, and problems with the optical identification of phase biaxiality are well known [17]. We have demonstrated it in a planar cell that imposes boundary conditions on the director, and these boundaries could also induce a biaxiality. However, the existence of \hat{n}_2 inversion walls and the continuous variation of the effective refractive index $n_{2,\text{eff}}$ across these walls shows that the biaxial state exists also in regions where the boundary anchoring of \hat{n}_2 is completely lifted, in the inversion wall centers. Moreover, the two states are observed in a

¹The optical result $n_3 < n_2$ does not necessarily imply $\varepsilon_{33} < \varepsilon_{22}$, but it is the case here.

homeotropic cell as well, where the N_u domains are black in the field off state while the N_b domains are characterized by a bright Schlieren texture (Fig. 7). Thus, we conclude that N_b is not merely a biaxial state in a thin planar cell but represents a biaxial nematic phase, induced by an electric field and stabilized in moderate (< 1 MV/m) fields.

We finally discuss some conditions for the appearance of the N_b state. The mesogens have to be sufficiently flat, but smectic order has to be absent. The bent-core unit of the twin mesogen is sufficiently anisotropic to match the first condition, and the rodlike unit suppresses the formation of smectic layers. A special feature of the mesogen studied here is the positive $\Delta\epsilon$, caused by the absence of large lateral dipole moments. This is a prerequisite for the splay FT in a planar cell, and it is essential for the electro-optic effects described here. Negative $\Delta\epsilon$ (lateral molecular dipoles) may provide even better conditions to induce N_b since such nematics favour \hat{n} perpendicular to \vec{E} . An electrical reorientation of the second director in a $\Delta\epsilon < 0$ material has been discussed, e.g. in [15]. In our samples, this effect is hidden by the alignment of \hat{n}_1 in the electric field.

References

- [1] M. Hird, *Liq. Cryst. Today* **14**, 9 (2005).
- [2] G. Pelzl, S. Diele, W. Weissflog, *Adv. Mater.* **11**, 707 (1999). A. Eremin, H. Nadasi, G. Pelzl, S. Diele, H. Kresse, W. Weissflog, S. Grande, *Phys. Chem. Chem. Phys.* **6**, 1290 (2004).
- [3] R. Amaranatha Reddy, C. Tschierske, *J. Mater. Chem.* **16**, 907 (2006).
- [4] H. Takezoe, Y. Takanishi, *Jap. J. Appl. Phys.* **45**, 597 (2006).
- [5] M.W. Schröder, S. Diele, G. Pelzl, N. Pancenko, W. Weissflog, *Liq. Cryst.* **29**, 1039 (2002).
- [6] C.V. Yelamaggad, S. Krishna Prasad, G.G. Nair, I.S. Shashikala, D.S. Shankar Rao, C.V. Lobo, S. Chandrasekhar, *Angew. Chem. Int. Ed.* **43**, 3429 (2004).
- [7] M.-G. Tamba, B. Kosata, K. Pelz, S. Diele, G. Pelzl, Z. Vakovskaya, H. Kresse, and W. Weissflog, *Soft Matter* **2**, 60 (2006).
- [8] R. Amaranatha Reddy, M.W. Schröder, M. Bodyagin, H. Kresse, S. Diele, G. Pelzl, and W. Weissflog, *Angew Chem* **117**, 784 (2005). M. Nakata, R.F. Shao, J.E. Maclennan, W. Weissflog, and N.A. Clark, *Phys Rev Lett.* **96**, 067802 (2006)
- [9] A. Eremin, S. Diele, G. Pelzl, W. Weissflog, *Phys Rev E* **67**, 20702 (2003).
- [10] W. Weissflog, M.W. Schröder, S. Diele, and G. Pelzl, *Adv. Mat.* **15** 630 (2003); W. Weissflog, H.N. Shreenivasa Murthy, S. Diele, G. Pelzl, *Phil. Trans. R. Soc. A* **364**, 2657 (2006).

- [11] J. Harden, B. Mbang, N. Éber, K. Fodor-Csorba, S. Sprunt, J.T. Gleeson, A. Jákli, *Phys. Rev. Lett.* **97**, 157802 (2006); *e-lc communications* (2006) http://www.e-lc.org/docs/2006_07_18_08_47_15
- [12] D. Wiant, J. T. Gleeson, N. Éber, K. Fodor-Csorba, A. Jákli and T. Tóth-Katona *Phys. Rev. E* **72**, 041712 (2005)
- [13] M.-G. Tamba, W. Weissflog, A. Eremin, J. Heuer, R. Stannarius (submitted)
- [14] L.J. Yu, A. Saupe, *Phys. Rev. Lett.* **45**, 1000 (1980).
- [15] B.R. Acharya, A. Primak, and S. Kumar, *Phys. Rev. Lett.* **92** 145506 (2004).
- [16] L.A. Madsen, T.J. Dingemans, M. Nakata, and E.T. Samulski, *Phys. Rev. Lett.* **92** 145505 (2004).
- [17] G.R. Luckhurst, *Nature* **430**, 413 (2004).
- [18] H. Gruler, and G. Meier. *Mol. Cryst. Liq. Cryst.* **16**, 299 (1972). H. Gruler, T. J. Scheffer, and G. Meier. *Z. Naturforschung*, **27a**, 966 (1972). H. Deuling. *Mol. Cryst. Liq. Cryst.* **19**, 123 (1972).
- [19] L. Leger, *Solid State Commun.* **11**, 1499 (1972); F. Brochard, *J. Phys. (France)* **33**, 607 (1972).